Journal of Marine Research, 56, 905–936, 1998

The effect of biogenic irrigation intensity and solute exchange on diagenetic reaction rates in marine sediments

by Robert C. Aller[1] and Josephine Y. Aller[1]

ABSTRACT

The activities of infaunal macrobenthos strongly influence the pathways, rates, and extent of organic matter remineralization and associated reactions in marine sediments. Solute transport during irrigation is a particularly important process that stimulates microbial activity and net remineralization, both within and adjacent to the bioturbated zone. Part of the stimulation proximal to the bioturbated zone is due to redox oscillation and oxidant supply during transport, but part of both the near and far-field effects are a result of other factors. Experiments designed to simulate different degrees of diffusive exchange, and thus infaunal abundances or activity, demonstrate a regular and strong dependence of anaerobic remineralization on diffusive transport. For example, net production of NH_4^+, $HPO_4^=$, I^-, and Mn^{++} increases as the effective distance between burrows becomes $\lesssim$2 cm (burrow abundance $\gtrsim$ 800 m^{-2}) in otherwise identical anoxic sediment. Corresponding changes in sedimentary bacterial numbers, exoenzyme activity, per cell growth rate (RNA), and solid phase properties (N, C/N, P) indicate that the increases in net rates are due in part to an absolute increase in total production. Transport-reaction models and experimental results demonstrate that relative decreases in the uptake of solutes into biomass, abiogenic precipitation reactions, and increased removal of inhibiting metabolites all occur simultaneously, enhancing both total and net remineralization. The phenonomenological first-order rate constant for organic matter decomposition is therefore a function not only of the reductant and oxidant pool properties, but also the environmental transport regime. Solid phase reaction products can differ substantially as a function of diffusive openness. For example, both organic P and the organic P/inorganic P ratio increase in more diffusively-open (irrigated) compared to diffusively-closed, anoxic sediment. The sensitivity of solute concentrations, microbial activity and diagenetic reaction balances to diffusive transport regime, indicates that macrofauna can functionally manipulate these properties through relatively small changes in burrow spacing patterns and individual burrow geometries.

1. Introduction

Benthic animal activities can influence both the absolute rates and relative balances of sedimentary decomposition reactions, often dramatically affecting net remineralization and synthesis patterns of new organic and inorganic compounds (Table 1). Irrigation of sediment during burrowing, feeding, and respiration is one particularly important factor controlling diagenetic reactions. By enhancing solute exchange between overlying water and pore fluids, irrigation supplies dissolved reactants from the water column, alters the

1. Marine Sciences Research Center, SUNY Stony Brook, Stony Brook, New York, 11794-5000, U.S.A.

Table 1. Macrofaunal effects on C_{org} decomposition/remineralization*.

Macrofaunal activity	Effect	Decomposition rate/extent**
Particle manipulation	Substrate exposure, surface area increase	+
Grazing	Microbe consumption, bacterial growth stimulation	+
Excretion/secretion	Mucus substrate, nutrient release, bacterial growth stimulation	+
Construction/secretion	Synthesis of refractory or inhibitory structural products (tube linings, halophenols, body structural products)	−
Irrigation	Soluble reactants supplied, metabolite build-up lowered, increased reoxidation	+
Particle transport	Transfer between major redox zones, increased reoxidation, redox oscillation	+

*(after: Aller, 1982, 1994; King, 1986; Andersen and Kristensen, 1991; Kristensen *et al.,* 1991; Alkemade *et al.,* 1992; Woodin *et al.,* 1993).

**(stimulation = +sign, inhibition = −sign).

spatial and temporal distribution of reactions, and lowers reaction product build-up in sediments. The resulting overall increase in the penetration of oxygen in bioturbated surface sediments, for example, clearly promotes aerobic metabolism and coupled redox reactions such as nitrification—denitrification (Rhoads, 1974; Jorgensen and Revsbech, 1985; Andersen and Kristensen, 1991; Pelegri *et al.,* 1994; Mayer *et al.,* 1995). Early quantitative studies of bioturbation and decomposition processes in organic-rich sediments demonstrated that net remineralization of organic matter, as reflected by ammonification, was also stimulated in anoxic regions both within or remote from the inhabited zone, implying that exchange of dissolved components other than oxygen during irrigation is a significant control on absolute rates of anaerobic metabolism and eventual organic matter burial (Aller, 1978; Aller and Yingst, 1985). Because diffusive transport is a strong function of spatial scaling of sources and sinks, such effects are expected to be dependent on the spacing and residence time of individual irrigated microenvironments and thus the average abundance, spacing, or burrowing activity of infauna (Fig. 1A). The purpose of the present study was to explicitly examine the dependence of anaerobic mineralization rates on diffusive exchange, further resolving one possible component of the dependence of net remineralization on macrofaunal population densities.

Assuming that burrow and tube boundaries are diffusively permeable (Aller, 1983), the characteristic scale of diffusion within the bioturbated zone is determined by the size and effective spacing of irrigated burrow structures. This characteristic scale (cm) can be roughly approximated by the annulus of sediment determined by burrow radii and inter-burrow spacing: $(r_2 - r_1) \sim (100/(\sqrt{\pi N}) - r_1)$, where N = effective animal abundance m^{-2}, r_1 = weighted average burrow radius (cm), and r_2 = weighted average half distance between burrow axes (cm). The expected approximate dependence of diffusion scale on burrow size and abundance within the bioturbated zone is shown in Figure 1B. The

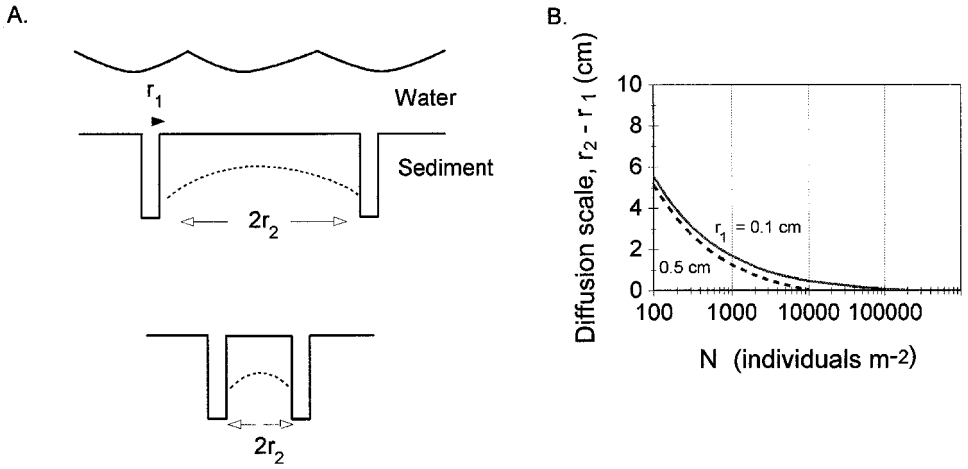

Figure 1. (A). Schematic cross-section of surface sediment illustrating total spacing scale ($2r_2$) between burrows. A maximum or minimum solute concentration (no net flux) occurs at half the distance (r_2) between any two identical irrigated burrows (concentration pattern illustrated by dashed line). (B). The characteristic diffusion scale ($\sim r_2 - r_1$) between uniformally distributed burrows varies with population abundance (N) and to a lesser extent with irrigated burrow radius (r_1).

effective value of N in these cases is obviously also a function of burrowing activity, individual burrow geometries, and irrigated tube formation rates. When considering the scales affecting strictly anaerobic regions, the value of the radius r_1 corresponds to the combined radius of a typical burrow and the surrounding oxidized zone. Abundance or effective burrow spacing dominates scaling (Fig. 1B). In the case of sediment immediately beneath the bioturbated zone, the vertical extent of the overlying irrigated region relative to the underlying interval being considered, is the transport scale of interest.

2. Methods

a. Experimental approach

Because the multiple effects of macrofauna on decomposition are simultaneous and normally inseparable (Table 1), we chose to isolate possible density-dependent scaling effects of diffusive exchange by experimentally varying the characteristic diffusive transport scales, and documenting the corresponding net reaction rates rather than manipulating specific macrofaunal populations per se. To do this, we used sediment plugs of varying thickness, L, to simulate different macrofaunal or diffusive source/sink spacings. The bottoms of the plugs were impermeable. Therefore, plug thickness L represents a diffusive transport scaling roughly equivalent to half the distance between any two identical burrow structures; where radial solute concentration gradients must approximate zero (i.e., no net diffusive flux at $\sim r_2$, Fig. 1). Sediment plugs were incubated in anoxic overlying water reservoirs having a known finite volume. The time-dependent concentra-

tions of components in the sediment pore water ($C(t)$), sediment solid ($\hat{C}(t)$), and overlying water ($C_T(t)$) are, in principle, redundant measures of net reaction rates (Fig. 2; see Aller and Mackin, 1989, for detailed discussion of technique).

Although the critical conceptual aspects of the experimental set-ups are depicted in Figure 2, different alterations were also used in the various experiments reported here. In some cases, instead of relatively small stoppered glass reservoirs inside a larger purged reservoir (Fig. 2), multiple sediment plugs having the same thickness, L, were openly immersed in a single large overlying water reservoir (see, e.g., Aller and Mackin, 1989). Continuous purging of overlying seawater with N_2/CO_2 maintained anoxic and pH conditions. A centrally-located magnetic stirring bar was either suspended above or placed at the bottom of the reservoir between plugs. In all cases, water-plug assemblies were kept in the dark, sometimes in a temperature-controlled incubator and/or a larger N_2/CO_2 purged glove box. The N_2/CO_2 stream was scrubbed of O_2 through Alltech O_2 indicating traps and passed through distilled water for humidification before entering the experimental reservoir. No O_2 was detectable in overlying water using either electrodes or Winkler titration measurements.

Sediment cores for experiments were collected at various times (1979–1996) from several nearshore shallow-water muddy sites: Mud Bay (Winyah Bay), South Carolina; Priest Landing (Skidaway Island), Georgia; Florida Bay (Bob Allen Key carbonate mud bank); and Long Island Sound (central), Connecticut/New York (Table 2). In all experiments reported here, sediment was first manipulated to remove macrofauna and subsequently homogenized. Visually obvious macrofauna were initially removed using tweezers, and sample intervals were forced through a 0.5 mm mesh nylon sieve without addition of water. The intervals used were generally below the surface oxidized layer (typical interval: 2–4 cm), and sediment was usually, but not always, handled at all stages under N_2 in a glove bag. Sediment was mixed by hand using a plastic spoon, placed into polycarbonate holders of known thickness (termed plugs), and the sediment surface smoothed flat with a stainless steel spatula. The plastic holders had sealed bottoms to prevent basal diffusion. Sediment plugs were placed into N_2/CO_2-purged, seawater reservoirs (polycarbonate or polyethylene) and incubated. The seawater used in each case was obtained at the sediment collection site and was initially depleted in nutrients relative to pore water (e.g., typically Cl- $\sim$ 0.4–0.65 (Florida Bay) M, NH_4^+ $\sim$ 1–5 μM, $HPO_4^= \sim$ 0.2–1 μM, $I_T \sim$ 0.3–0.4 μM, $\Sigma CO_2 \sim$ 1.8–2 mM, $Mn^{++} <$ 0.05 μM, pH 7.8–8.2). For many experiments, a portion of the homogenized sediment was also placed into polyethylene centrifuge tubes, sealed, and incubated under N_2/CO_2 without access to a fluid exchange reservoir. Diffusion plugs with overlying water reservoirs are referred to here as **'open'** incubations and the tube time-series incubations are referred to as **'closed.'**

In most cases, plugs were sampled for pore water ($C(t)$) and solid phase ($\hat{C}(t)$) composition after a set incubation period of 5–10 days. Overlying water was generally sampled periodically during plug incubations using a syringe/tubing assembly, providing an estimate of $C_T(t)$. In one set of experiments, PL95-1, a time series of plug incubations

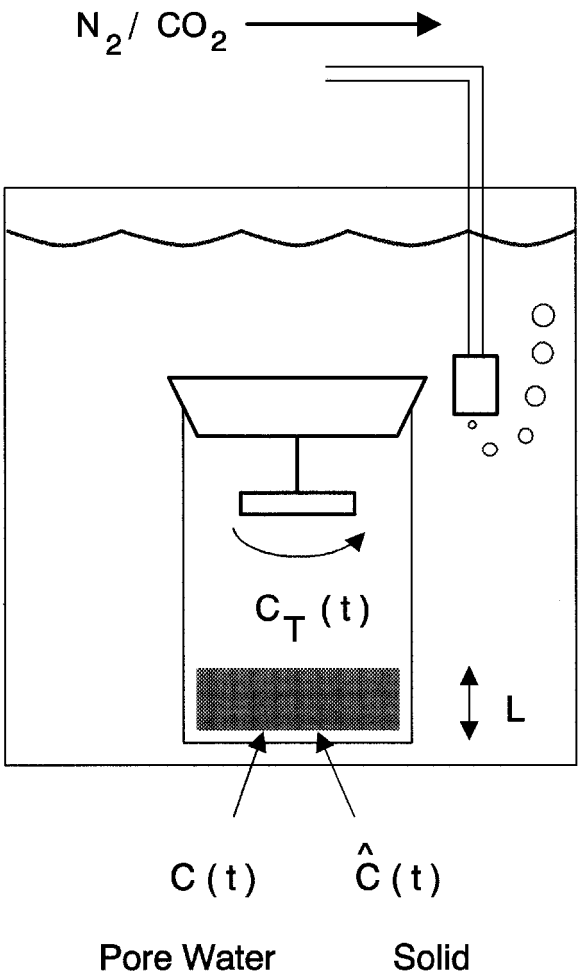

Figure 2. Typical experimental incubation set-up illustrating sediment plug diffusion scale (sealed bottom at L) and the concentration measurements utilized to estimate net reaction rates within sediment. The impermeable base results in a maximum or minimum solute concentration at L (no net flux) comparable to that occurring midway between identical burrow diffusive sinks (Fig. 1A).

set-up as depicted in Figure 2 were sampled after 7, 20, 34, 48, and 61 days. Overlying water in that case was changed approximately every 2 weeks in the outer purged reservoir and independent internal plug reservoirs were opened and exchanged. In a second long term series, PL96-1, relatively thin (0.17 cm) and thick (1.4 cm) plugs were incubated in a single reservoir and sampled periodically over ~120 days. In most experiments, closed incubations were sampled at multiple times during the corresponding periods of open plug incubations, providing an estimate of net reaction rates under diffusively closed conditions.

Table 2. Experimental schedule and sediment sources.

Experiment	Site	Date	Temperature	Depth intervals (cm)
PL81-1	Mud Bay, SC	3/17/81	12	0–1, 3–5, 13–15
PL81-6	Mud Bay, SC	8/31/81	26	0–1, 3–5, 10–12
PL81-9	Mud Bay, SC	10/5/81	26	0–1, 1–2, 3–5, 10–12
PL84-1	Skidaway Is., GA	8/1/84	25	3–5
PL84-2	Skidaway Is., GA	8/21/84	25	3–5
PL85-2	Skidaway Is., GA	7/27/85	25	3–5
PL85-3	Skidaway Is., GA	8/10/85	25	3–5
PL88-1	LIS	6/9/88	12.5	2–6
PL88-3	Florida Bay, FL	7/21/88	31	2–6
PL91-2	LIS	7/5/91	18.5	2–4, 10–12
PL91-3	LIS	11/21/91	18.5	2–4
PL92-1	Florida Bay, FL	6/16/92	28	0–2
PL92-2	Florida Bay, FL	7/5/91	28	0–2
PL92-3	LIS	7/27/92	15	2–4
PL92-4	LIS	9/13/92	20	2–4
PL95-1	LIS	6/15/95	22.5	0–2
PL96-1	LIS	4/19/96	22.5	3–4

b. Sampling and analytical methods

Water samples were usually obtained at several times during an incubation. Overlying reservoir water was collected in plastic syringes and filtered through inline polycarbonate filters (0.4 μm pore size) directly into vials. At the end of a plug incubation period, the sediment-overlying water assembly was placed in a N_2-filled glove bag and plugs were retrieved for analysis using stainless steel forceps. A small portion of sediment from plug or tube incubations was removed for bacteria counts and in some cases ATP concentrations, per-cell growth rate (based on ribosomal RNA, rRNA), and potential hydrolytic enzymatic activity analyses. Pore water was separated from the remaining sediment by centrifuging sediment (plugs, tubes) or by squeezing sediment within plastic syringes (plugs). In the case of centrifuged samples, sediment was rapidly transferred under N_2 into tubes, centrifuged at 5000 rpm for 5 minutes, the supernatant removed into a syringe, and filtered through an inline filter as for overlying water. Syringe squeezers were also filled under N_2 and the pore water passed directly through nylon screen and inline filters into a receiving syringe. Pore water was either refrigerated, frozen, or acidified, depending on the subsequent analysis to be performed. The latter technique allowed more rapid handling with a total processing time after removal from the overlying water reservoir of $\lesssim$5 minutes. After pore water removal, sediment was frozen for possible later solid phase analyses.

Dissolved constituents in pore and overlying water were analyzed using the following techniques: NH_4^+-indophenol blue (Solorzano, 1967) or flow injection gas diffusion (Hall and Aller, 1992); ΣCO_2-flow injection gas diffusion (Hall and Aller, 1992); Mn^{++}-atomic adsorption or formaldoxime (Goto *et al.,* 1962), $HPO_4^=$-molybdate blue (Strickland and

Parsons, 1968); and I_T (total $I \sim I^-$-Ce/As catalytic method. Analytical precision of dissolved constituents was typically ~3%. Adsorbed NH_4^+ was measured by displacement with 2N KCl (Rosenfeld, 1979; Mackin and Aller, 1984). Lysable NH_4^+ was defined as the difference between KCl extractable NH_4^+ before and after freezing of sediment (Aller, 1994). Solid phase exchangeable P utilized displacement by 1M $MgCl_2$ (Ruttenberg, 1992); total P and organic P were obtained by 1N HCl 16 hr leaches at 22° C of ashed (450° C) and unashed sediment respectively (Aspila *et al.,* 1976; Ruttenberg, 1992). The operational terminology adopted here is that of Aspila *et al.* (1976) and Ruttenberg (1992); although it is clear that the 'inorganic' P pool (P_{inorg}) also includes the most labile organic P forms, and the 'organic' P pool (P_{org}) contains not only refractory organic but also unreactive inorganic components. Typical precisions were ~5–7%. Total sediment C and N were measured using a Fisons instruments Model 1106 CNS analyzer. Typical precisions were 2–3% and 3–5% for C and N respectively. Not all measurements were made in every experiment.

Sediment and overlying water (unfiltered) bacteria samples were fixed in 3% formalin and cells counted using acridine orange epifluorescence following Watson *et al.* (1977) (precision <5%). Bacterial exoenzyme activity was estimated in experiment PL95-1 by incubation of samples with fluorogenic enzyme substrate analogs (MUF-galctoside, MUF-palmitate, leucine-MCA) utilizing techniques described in Boechker and Cappenberg (1994), Hoppe (1993), Meyer-Reil (1986), and Chrost (1991) specifically modified for small sample sizes. Sediment subsamples from plugs and closed tubes were injected with fluorescent substrates and incubated anoxically (under N_2) for 2–4 hours. ATP concentrations were measured by extracting sediment with boiling phosphate-citrate buffer (Bulleid, 1978), followed by luciferin-luciferase luminescence assay. Concentrations were corrected for extraction efficiency and chemical interference as a function of sample weight. All bacterial counts and ATP concentrations were normalized to dry weight sediment. rRNA measurements followed the procedures outlined in Kemp *et al.* (1993) and Lee *et al.* (1993) with an initial sonification step to isolate intact preserved cells from the sediment. In brief, diluted formalin-preserved sediment samples were vortexed, sonicated, centrifuged, the supernatant removed, remixed, sonicated, and centrifuged. The pelletized cells were resuspended in 0.1% Nonidet P-40 (Sigma) and incubated overnight at 4°C to increase cell permeability. Following removal of supernatant, cells were applied to microscope slides coated with a gelatin solution. The smear was dried at room temperature, dehydrated by sequential ethanol baths, and dried again at room temperature. Cells were then hybridized with fluorochrome-labelled oligonucleotide probes, and the resulting cell fluorescence measured with an image analysis system. The suite of probes used were developed by Lee *et al.* (1993) to yield predictable increases in fluorescence in direct proportion to increasing rRNA content in intact, individual cells. The probes used in the mixture were 2 universal and 3 bacterial, and were designed to target all true bacteria (sensu Woese, 1987). Other cells were visually screened on the basis of size and shape.

c. Reaction rate calculations

Net reaction rates for dissolved components in sediment plugs were estimated in several ways. Assuming a constant whole sediment diffusion coefficient, D_S, a constant average reaction rate, R, and ignoring consumption or production in the overlying water during the period of incubation, then:

$$\frac{\partial C}{\partial t} = \frac{D_S}{1+K}\frac{\partial^2 C}{\partial x^2} + \frac{R}{1+K} \qquad \text{and} \qquad \frac{\partial C_T}{\partial t} = \frac{A}{V_T}\varphi D_S\left(\frac{\partial C}{\partial x}\right)_{x=0} \tag{1a,b}$$

where:

C = pore water solute concentration (mass/volume pore water)
C_T = overlying water solute concentration
R = net reaction rate (mass/volume pore water/time)
D_S = whole sediment diffusion coefficient
K = reversible linear adsorption coefficient
t = time
x = depth in plug, origin at plug surface, positive axis into sediment
A = area of plug surface
V_T = volume of overlying water
φ = sediment porosity

The analytical solutions to these equations with initial and boundary conditions:

$$\begin{aligned} &t = 0, \qquad C(0 \le x \le L) = C_o \qquad C_T = C_{To}; \\ &t > 0, \qquad x = 0, \qquad C = C_T; \qquad x = L, \qquad \partial C/\partial x = 0 \end{aligned} \tag{2}$$

are given in Aller and Mackin (1989). Explicit and implicit finite difference numerical schemes were also used to evaluate time-dependent behavior of both the overlying reservoir and sediment plug solutes. In many practical instances where C_T changes only a small amount relative to C (i.e., V_T relatively large), after a short time depending largely on L, D_S, and C_o, the following steady state relation holds:

$$C_{ss} = C_T + \left(\frac{L^2}{3D_S}\right)R \tag{3}$$

where: C_{ss} = average steady state concentration in plug of thickness L.

Under such conditions the pore water concentration in the sediment plug is readily related to the net reaction rate. This simple relation held for most cases considered in the present experiments where plug sets were typically sampled within 7–10 days after initiating an experiment. Note that in thin plugs, for example $L = 0.5$ mm, steady state is essentially achieved within a few minutes whereas thicker plugs, for example $L = 2$ cm can require as much as a week, depending on initial conditions and reaction rate. Exact calculations were generally used to determine R in the case of plugs $L > 1$ cm, although there was usually little practical difference between such calculations and those predicted

from Eq. (3). In all cases, diffusion coefficients were estimated from the relation $D_S \sim \varphi^2 D_o$ (Berner, 1980; Ullman and Aller, 1982), where φ = porosity calculated from water content (assumed particle density 2.6 g cm^3) and D_o is the free solution diffusion coefficient at the appropriate temperature and salinity (Li and Gregory, 1974).

Ignoring consumption or production in the overlying water and reversible adsorption on sediment, the time rate of change in the concentration of a solute in overlying water over a particular time period is related to the average production or consumption rate, R, in the sediment plug:

$$dC_T/dt \sim (A/V_T)\varphi RL. \tag{4}$$

Ignoring reversible adsorption for solutes such as NH_4^+ is a good assumption after an initial period of rapid desorption from sediment plugs, and for situations in which the overlying water concentration remains significantly lower than pore water. An integrated form of Eq. (4) can also be used over specific time intervals, or the exact solutions to Eqs. (1) and (2) can be used for the most accurate calculations.

In the cases of closed incubations, the net reaction rate for a specific solute under consideration is assumed to be given by:

$$dC/dt = R/(1 + K). \tag{5}$$

The concentration time dependences for solutes subject to zeroth order kinetics are essentially linear over the generally short time periods used here. For longer term experiments, linear approximations for concentration time dependences over specific time intervals were used to derive average reaction rates corresponding to those intervals.

3. Results

a. Relation of solute reaction rates with diffusion scale

The net ammonification rates calculated from pore and overlying water concentration differences (Eqs. 1–3) typically varied regularly with sediment thickness or diffusion scale (Fig. 3). Calculated rates for plugs of ~2–3 cm were usually experimentally indistinguishable from closed incubation estimates. Rates increased slightly but perceptively above closed incubation rates (~1.2–2×) when diffusion scales were between ~2–0.5 cm. At scales <0.5 cm, however, relatively strong, near exponential relative increases (>5×) occurred. Because diffusion scale and pore water-overlying water concentration differences were proportional in these instances, calculated rates also varied inversely with NH_4^+ pore water concentration (Fig. 3B). Both the general range of measured ammonification rates and the rate-diffusion scale relationships were similar at the various shallow water sediment source sites, all of which had comparable organic matter contents (1–2% C_{org}).

Additional pore water components derived from organic matter decomposition also showed evidence of changes in net remineralization rate as a function of diffusion scale.

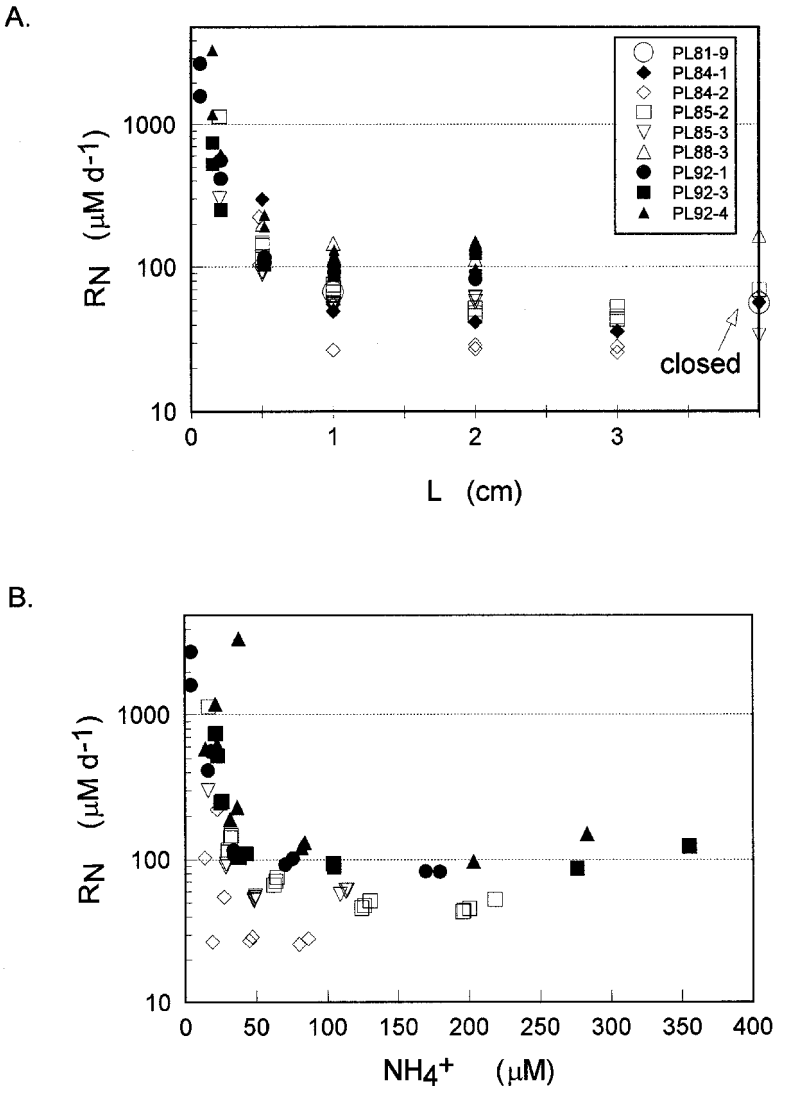

Figure 3. (A). Examples of relationship between relative rates of net NH_4^+ production calculated from pore water—overlying water concentration differences, and sediment diffusion scale *L*. The relative patterns of increasing net rate with decreasing *L* are similar in a wide range of nearshore sediments. Closed incubation rates (corrected using measured linear absorption coefficients) are arbitrarily plotted at $L = 4$ cm. (B). Net rates of NH_4^+ production relative to pore water concentration rather than *L*.

Calculated rates of $HPO_4^=$ and I_T production increased inversely with diffusion scale, although not always as dramatically as did NH_4^+ (Fig. 4). Pore water-overlying water differences in ΣCO_2 were often too small to allow analytically accurate calculations from Eqs. (1–3), however, net fluxes into overlying water and rates derived from Eq. (4)

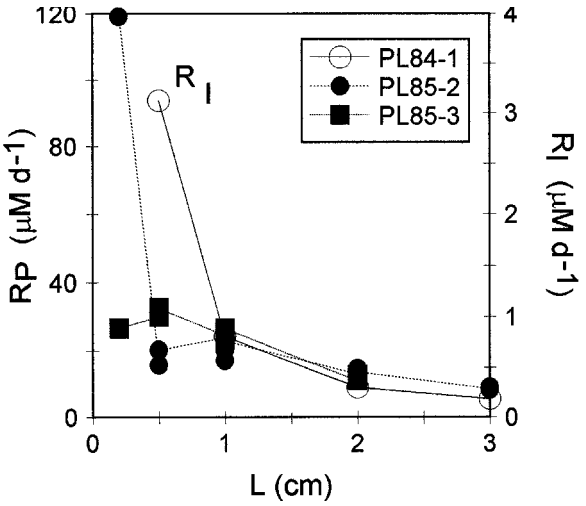

Figure 4. $HPO_4^=$ and I^- also tend to have relative increases in calculated net production rate at decreased diffusion scales L.

indicated that in at least some cases (measurements not always made) net C_{org} remineralization as measured by ΣCO_2 release also increased as diffusion scale decreased (Fig. 5). The relative importance of different possible pathways of decomposition and ΣCO_2 generation were not determined. Dissolved Mn^{++} release and in some cases discernible sulfide production (ΣH_2S and/or blackening of sediment by FeS) implied the occurrence of both metal oxide and $SO_4^=$ reduction.

The net production of Mn^{++}, a direct or indirect product of suboxic, anaerobic decomposition, varied with sediment plug thickness. Estimates of net production as

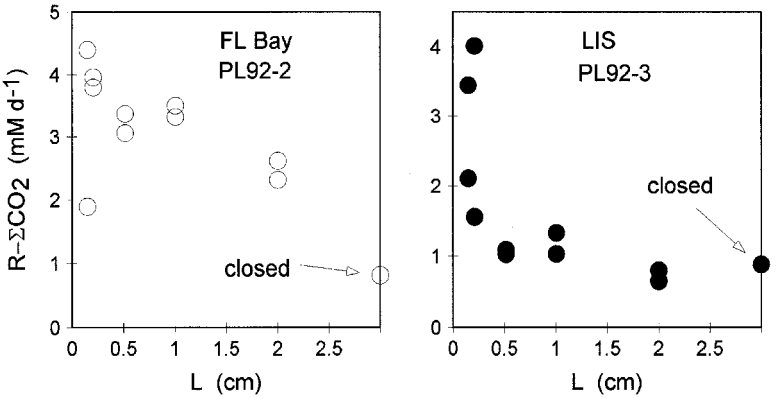

Figure 5. The net sedimentary production rate of ΣCO_2 calculated on the basis of net flux into overlying water ($C_T(t)$) also increases with decreasing L as shown by examples from Florida Bay and Long Island Sound. The relative increase in remineralization is less than calculated for NH_4^+ on the basis of pore water concentration. Closed sediment incubation rates are plotted at $L = 3$ (arbitrary) for comparison.

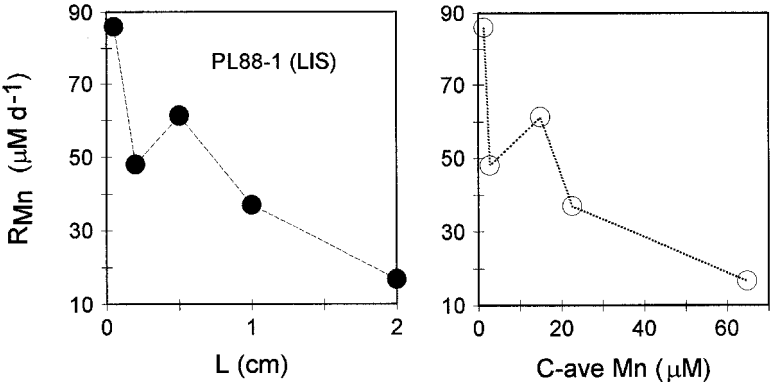

Figure 6. Relative rates of sedimentary net Mn^{++} production calculated on the basis of net flux into overlying water ($C_T(t)$) increase with either decreasing diffusion scale or average pore water concentration.

calculated by net flux into overlying water (Eq. 4), showed regular increases with decreases in diffusion scale or average pore water concentration (Fig. 6).

Possible production of Fe^{++} was not measured. Dissolved ΣH_2S was analytically detectable only in the carbonate sediments from Florida Bay (plug pore water range $\sim$2 μM − 1.4 mM, results not presented).

b. Time dependence of net reaction rates

Long-term, time-series experiments indicated that all calculated net reaction rates tended to decrease with time, but that time-dependent attenuation of rates differed between closed and open systems. Results from PL96-1 indicated that calculated net ammonification rates (Eqs. 1–3; 5) were higher the more open the sediment to solute exchange (decreased diffusion scale), and attenuated less with time than rates calculated from closed incubations (Fig. 7). The nearly comparable rates from the closed incubation and the thickest sediment plug (1.4 cm) at $t = 0$, demonstrates that the operationally measured linear adsorption coefficient used in these calculations is reasonable (i.e., PL96-1 K = 0.65 from KCl displacement of NH_4^+, $\varphi = 0.757$; same technique used in other incubation comparisons; general measured K range 0.65 − 1.7).

The net production rate of pore water Mn^{++} also attenuated with time in long-term, time-series experiments, as shown by results from PL95-2, which used the overlying water net fluxes and estimated rates from model Eq. (4) (Fig. 8). As in the shorter-term experiments, net production was highest at the smallest diffusion scales (Mn^{++} concentration), but in contrast to NH_4^+, the attenuation of the net production rate with time was highest in the thinnest sediment plugs (Fig. 8A).

c. Solid phase reactant/product patterns

Most of the experiments performed here were too short in duration to allow analytically significant changes to occur in bulk solid sediment properties such as C_{org} or total N

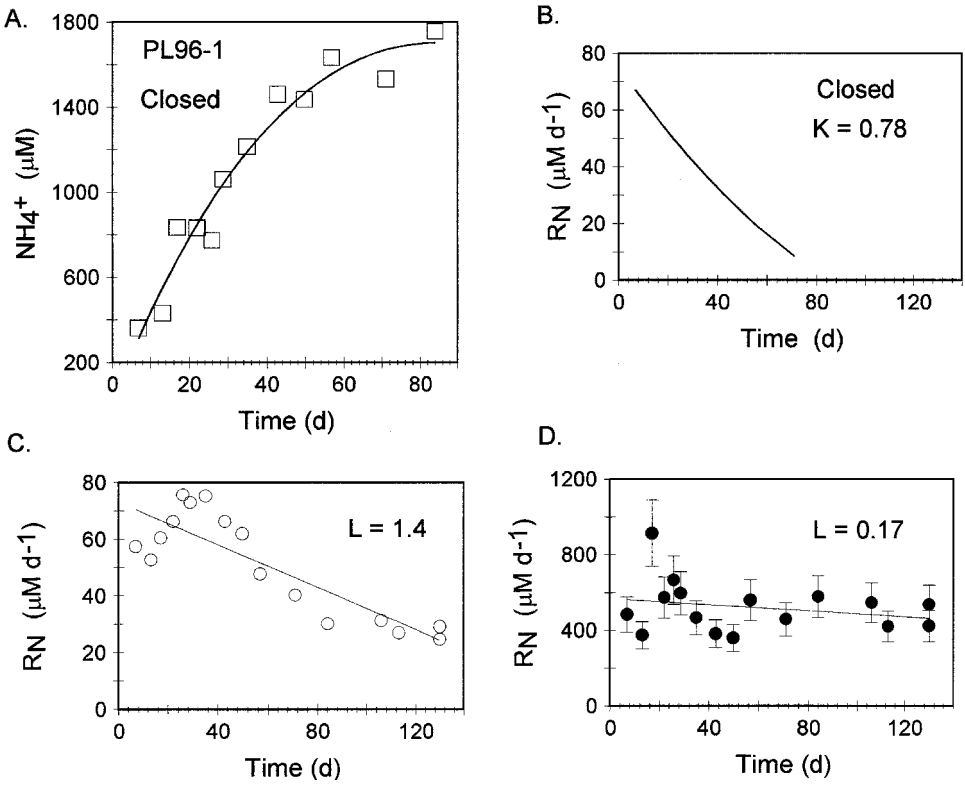

Figure 7. (A). PL96-1 (LIS) NH_4^+ pore water concentration versus time of closed incubation in LIS sediments. The curve is a least squares polynomial fit. (B). Net production rate of NH_4^+ in closed incubation as a function of time (derivative of polynomial fit from (A)). The measured linear adsorption coefficient, $K = 0.65$, was used to correct for adsorption losses. (C). Net production of NH_4^+ in PL96-1 sediment plugs having $L = 1.4$ cm as a function of incubation time. (D). Calculated NH_4^+ production in sediment plugs with $L = 0.17$ cm as a function of time. The error bars represent uncertainty in the calculation based on uncertainty in plug thickness. Calculated production rates are higher and attenuate less with time as diffusive openness increases.

(Fig. 9). Even slight heterogeneity between plugs significantly compromises patterns; however, PL96-1 was sufficiently long that changes were discernible, and could be compared to solute-based rate calculations or reveal additional processes. The C_{org}/Total N ratio, which damps solid phase heterogeneity somewhat, tended to increase regularly with time (Fig. 10). The thinnest plugs (0.17 cm) showed the greatest relative increase (overall time series C/N averages: 10.6, 9.5, and 9.6 for $L = 0.17$, 1.4, and closed). Although there was considerable scatter, there was a tendency for total N to decrease with time in the thinnest plugs. A least-squares linear regression to the data gives an overall slope corresponding to an NH_4^+ production rate of $\sim$70 μM d^{-1} ($y = 0.00011x + 0.191$, $r = 0.71$; $P < 0.002$), if the two points with greatest departure from the apparent overall

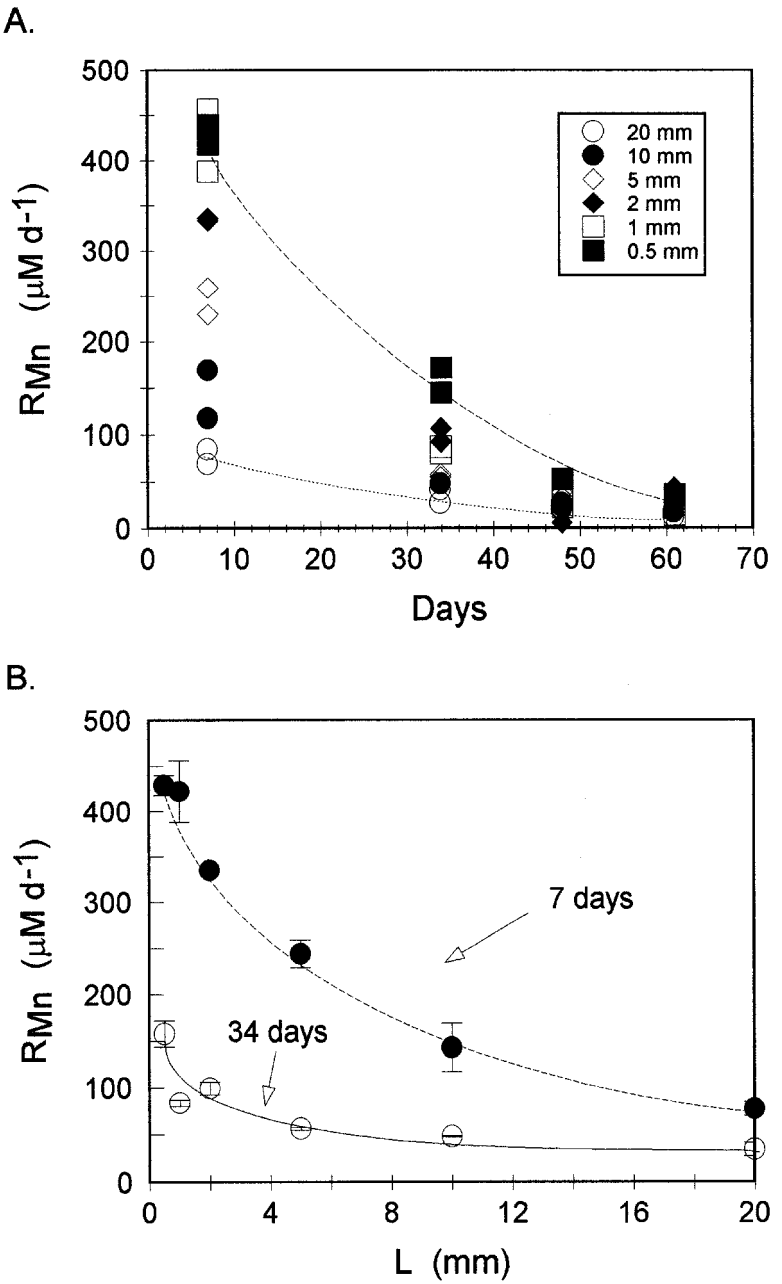

Figure 8. (A) PL95-1 (LIS) net production rate of Mn^{++} ($C_T(t)$ flux based estimates) as function of time and sediment diffusion scale (L). (B) Attenuation of net production rate of Mn^{++} ($C_T(t)$ flux based estimates) as function of diffusion scale, L, after different periods of incubation (7, 34 days).

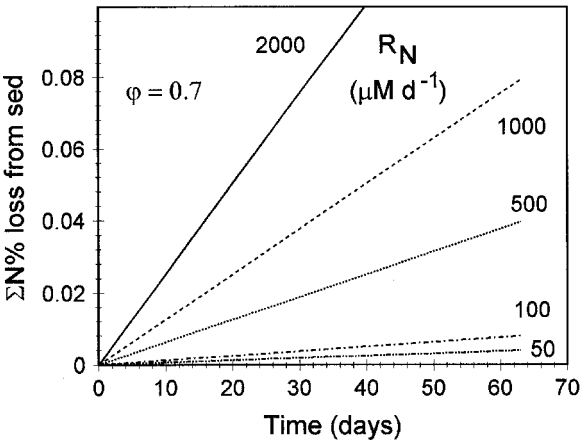

Figure 9. Predicted cumulative loss of solid phase N as a function of time and different sustained net production rates of NH_4^+, R_N (μM d^{-1}). Solid phase N losses are analytically undectectable for most experimental periods and ranges of net production rates.

trend are ignored. This value is ~6× smaller than the average solute modeled rate for the thinnest plug, but is ~2–4× the rates calculated for either the thicker plug (1.4 cm) or closed incubation series.

Significant differences in the behavior of solid phase P were found between open and closed incubation series, and also with the scale of diffusive openness. In PL96-1, the closed incubation tended to have slightly higher total P (ΣP), higher 'inorganic P,' and

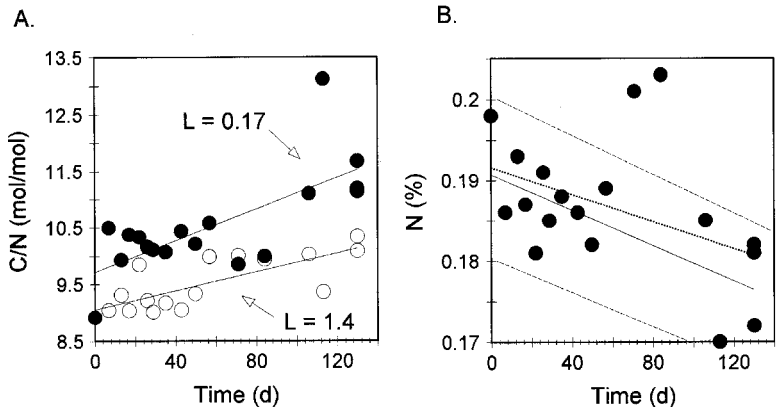

Figure 10. (A). Solid phase C/N ratios as function of time in PL96-1 (LIS). The thinnest plugs showed tendency for greatest increase with time ($L = 0.17, r = 0.7, P < 0.001$; $L = 1.4, r = 0.82$, $P < 0.001$). (B) Solid phase weight %N as function of time in $L = 0.17$ cm plugs. The least squares line fit (solid) utilizes only those points within the dashed line envelope ($r = 0.71$, $P < 0.002$). The dotted line fit utilizes all points ($r = 0.4$, $P < 0.06$). The closed incubations showed no tendency for a time dependent pattern for either C/N or N.

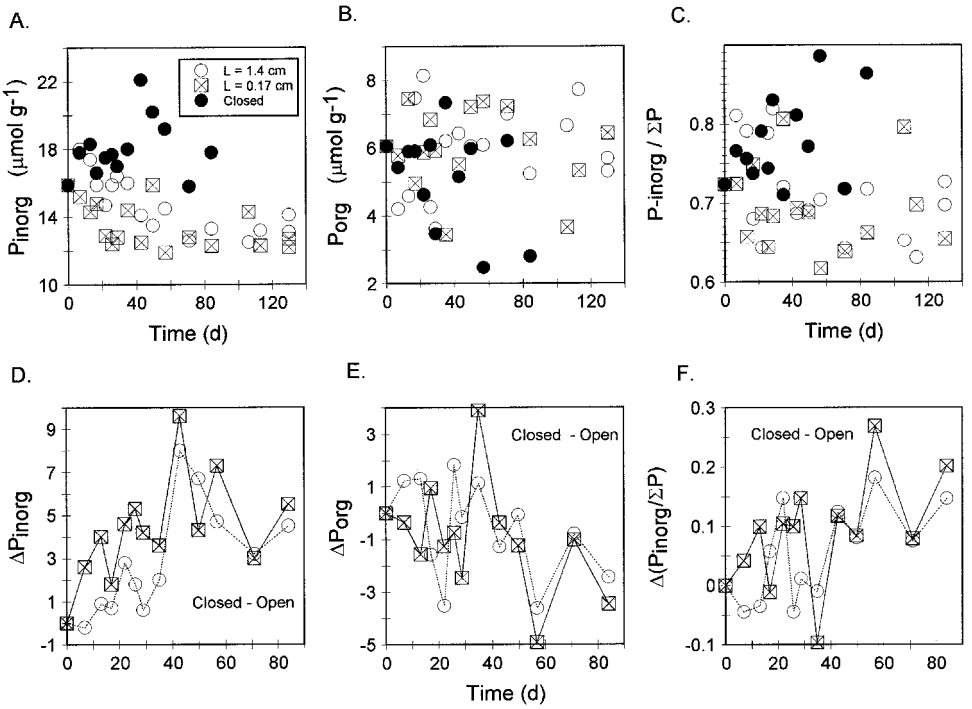

Figure 11. As illustrated by PL96-1 (LIS) there are distinct differences in the solid P inorganic and organic pool distributions with time as a function of transport scale (anoxic conditions). (A) Inorganic P (labile inorganic and organic). (B) Organic P (refractory organic and inorganic). (C) Fraction of total P in the inorganic P fraction. (D) Difference between inorganic P in closed and open incubations as a function of time (closed value minus respective plug value at specific time). (E) Difference between orgnanic P in closed and open incubations as a function of time. (F) Difference between inorganic P fraction in closed and open incubations.

lower organic P than diffusively open sediment (Fig. 11). The ratio of $P_{inorg}/\Sigma P$ was also higher in the closed than open incubations, with the lowest overall ratios in the most diffusively open sediment (thinnest plugs) (Fig. 11). Diffusively open sediment had overall higher concentrations of P_{org} than did diffusively closed. The thinnest plugs (0.17 cm) diverged substantially from the thicker plugs (1.4 cm) during the first ~30 days of incubation, but properties converged thereafter. As demonstrated by the PL95-2 time series averages (~60 d), the exchangeable P pool ($MgCl_2$ extraction) also differs as a function of diffusive scale, with smallest exchangeable P concentrations in the most diffusively open sediment (thinnest plugs) (Fig. 12).

In PL96-1, leachable solid Mn (1N HCl) averaged 10, 5.4, and 2.7 μmol g^{-1} for closed, 1.4 cm, and 0.17 cm plug incubations, demonstrating greatest net loss of Mn from the most diffusively open sediment.

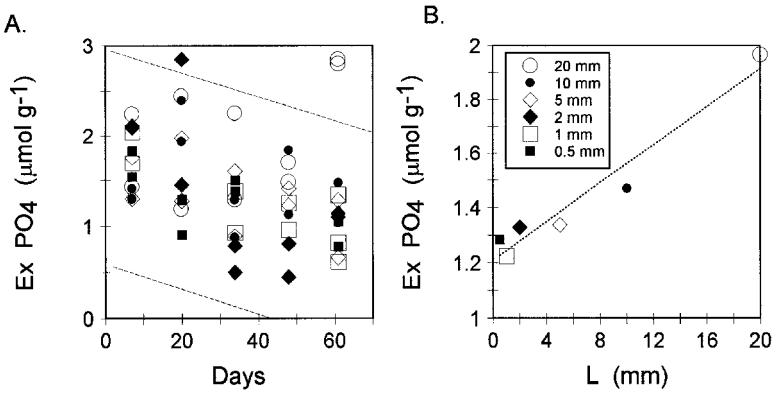

Figure 12. (A). As shown by PL95-1, exchangeable $HPO_4^=$ ($MgCl_2$ extractable) in sediment decreases with time of incubation (reaction) and as a function of diffusive openness. (B) Mean value of exchangeable P over ~60 days of incubation varies as a function of transport scale (L), with smallest exchangeable P in the thinnest sediment layers.

d. Measures of bacterial growth and activity

Several measures of bacterial biomass or activity indicate that metabolic activity was highest in diffusively open, compared to diffusively closed, sediment. Total bacteria and ATP were typically elevated in open versus closed incubations (Figs. 13, 14). Lysable NH_4^+, the differential amount of exchangeable NH_4^+ released from sediment by 2 N KCl before (exchangeable) and after freezing, was also higher in most diffusively open samples, increasing rapidly with decreasing diffusion scale L (Fig. 15). Lysable NH_4^+ apparently reflects both microbial biomass and remineralization activity (Aller, 1994). RNA fluorescence per cell indicated distinctly highest values in the thinnest sediment layers, consistent with greatest cell synthesis activity at smaller diffusion scales (Fig. 16). The cellular RNA differences likely correspond to a ~2–5× higher growth rate in the thinnest compared to the thicker plugs (Kemp, 1995). Although there is substantial experimental scatter, exoenzyme activity (PL95-2) for MCA-leucine and MUF-palmitate showed a tendency for the highest values to occur in the most diffusively open sediment during the first ~20 days of incubation (Fig. 17).

4. Discussion

a. Net remineralization patterns

The calculated net remineralization rates for NH_4^+, $HPO_4^=$, and $I_T(\sim I^-)$, based on pore water-overlying water concentration gradients indicate that net production rates increase dramatically as diffusion scale (sediment thickness) decreases and efficiency of solute exchange with overlying water increases (Figs. 3, 4). It is possible that part of this apparent trend results from experimental and analytical artifacts, although artifacts are not likely to be exclusive factors. Because the rate calculations using model equations (1–3) are based

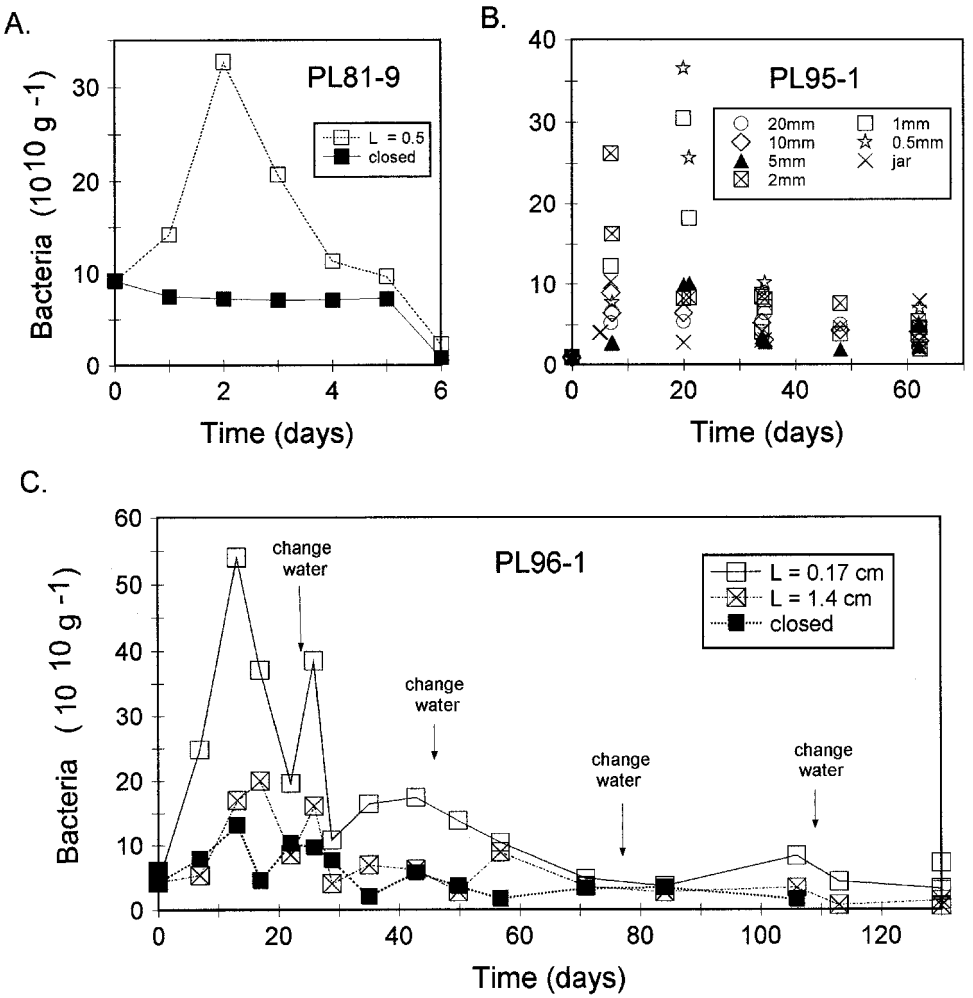

Figure 13. Bacteria abundances are typically higher, at least during initial periods, in diffusively-open (irrigated) compared to closed sediment. (A). Time series bacteria abundance in sediment from Mud Bay, SC (L = 0.5 cm, 0–1 cm sediment interval). (B). Time series bacteria abundances in LIS sediment having various L values (PL95-1). (C) PL96-1 (LIS) time series. Relatively elevated bacterial abundances are maintained in the most diffusively open sediment (L = 0.17 cm) for months, although greatest differences are found during the first few weeks.

on concentration differences that become small as sediment thickness decreases, analytical uncertainty increases with decreases in sediment thickness. The relative rate-scale patterns are systematic, however, implying that random analytical errors are an unlikely cause. Slight contamination of filters or sample vials might explain systematic patterns in isolated instances (e.g., NH_4^+), but contamination is an unlikely determinant in multiple cases or for multiple solutes. Handling time was also minimized (a few minutes in most instances)

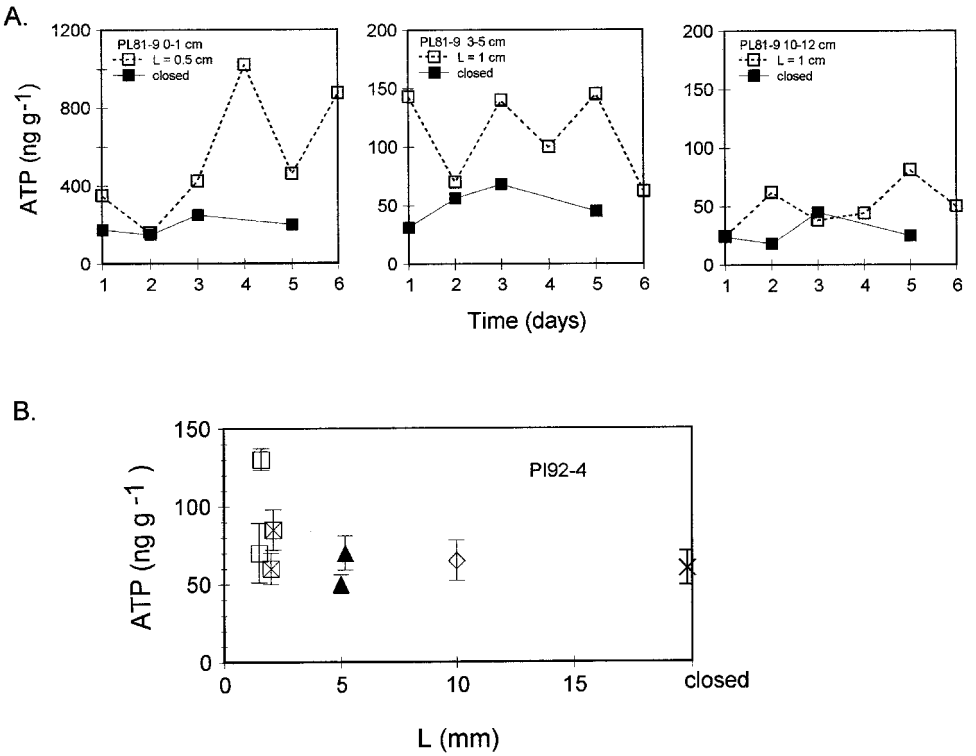

Figure 14. ATP (combined biomass and activity indicator) tends to be elevated in diffusively open relative to more diffusively closed sediment. (A) Time series ATP in PL81-1 (Mud Bay, SC) from different sediment intervals. All sediment intervals (0–1, 3–5, 10–12 cm) responded to differences in diffusive openness. (B) Relative ATP pattern in PL92-4 (LIS) plugs after 5 day incubation.

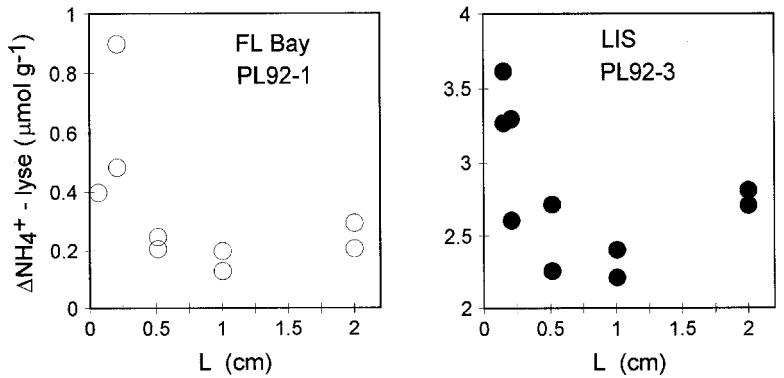

Figure 15. The lysable NH_4^+ pool (difference between KCl extracted NH_4^+ before and after freezing sample) increases with decreases in diffusion scale, indicating increased labile NH_4^+ storage.

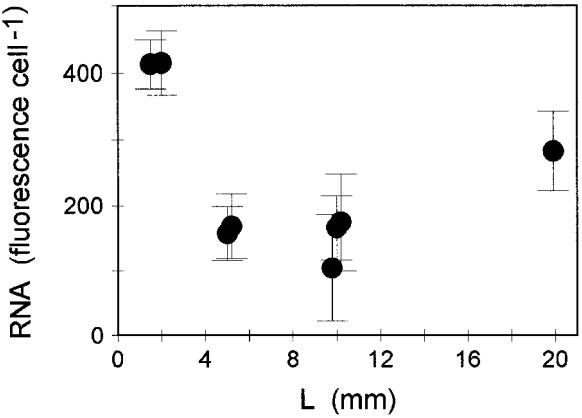

Figure 16. A tendency for increased RNA in bacterial cells as diffusion scale decreases is consistent with greater per cell synthesis (~2–5×) as L becomes smaller (PL92-4).

to reduce the effect of possible rapid pore water concentration changes after removal of sediment from overlying water reservoirs. A more serious contributing error factor is the presence of diffusive boundary layers, which have been assumed insignificant in the model derivations and calculations of equations (1–3) (Santschi *et al.,* 1991).

The effect of diffusive boundary layers of various thickness can be explicitly taken into account in estimations of rates by assuming that stagnant layers having no reaction overlie sediment. In such a case, the concentration differences between sediment and overlying water are a function not only of sediment diffusion and reaction rates, but also boundary layer thickness and the ratio of free solution to sediment diffusion coefficients. Let the apparent calculated net remineralization rate be: $R = 3D_s(C_{ss} - C_T)/L^2$ as defined by the

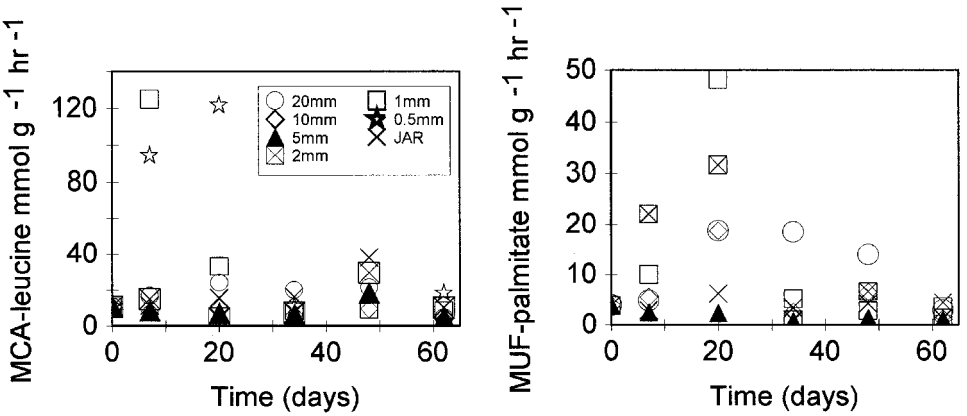

Figure 17. The highest leucine and palmitate exoenzyme activities tend to be in the thinnest sediment layers during initial (several weeks) periods of incubation, consistent with generally increased bacterial metabolic activity in diffusively-open sediment.

steady state equation (3) assuming no significant boundary layer. If a diffusive boundary layer of thickness L_B actually is present, the correct steady state relation between the actual net rate, R^*, and sediment-overlying water concentration differences is:

$$R^* = R/[1 + 3\varphi^3(L_B/L)] \tag{6}$$

Where R is defined by Eq. (3) and $D_s = \varphi^2 D_o$.

The relative calculation error made by ignoring the possible presence of diffusive boundary layers increases dramatically as sediment and diffusive boundary layer thicknesses become comparable. The ratio, R/R^*, represents the factor by which the apparent reaction rate might be overestimated in such an instance, and has the same basic functional form and relative magnitudes with respect to L (sediment thickness) as do the calculated apparent remineralization rates (Fig. 3, Fig. 18).

There are a number of reasons to believe that, although diffusive boundary layers must contribute to and accentuate the calculated relative pattern at small L, the apparent increases in rates with decreasing diffusive scale are largely real. First, the patterns were repeatable under a variety of stirring conditions and experimental setups, several of which were agitated to near particle resuspension levels. Second, attempts in some cases at direct measurement of the diffusive boundary layer using oxygen microelectrodes (e.g. Jørgensen and Revsbech, 1985) indicated thicknesses $\lesssim$0.1 mm and minor effects on calculations for sediment thickness $\gtrsim$1–2 mm. Third, the flux-based estimates of relative rates (Eq. 4) show the same basic relative patterns, and for the constituents measured are not dependent at steady state on diffusive boundary layers. Fourth, the behavior of solid phase properties is different as a function of diffusive openness, consistent with relative rate differences. And, fifth, indicators of microbial activity imply regular variation as a function of diffusive lengthscale, activity increasing as solute exchange increases.

The increase in net remineralization rates with increasing solute exchange therefore demonstrates directly that irrigation of sediment by infaunal benthos can result in a macrofaunal density-dependent increase in net remineralization, microbial activity, and sediment-water solute fluxes of constituents not normally considered sensitive to concentration dependent reactions (e.g. Figs. 1, 3). The functional dependence on transport scaling indicates that effects are relatively modest (e.g., 1.3×) over a large range typical of average scales in many benthic communities, but become increasingly important at small scales or, equivalently, close spacing between groups of individuals or burrow sectors. Organic-rich regions near the sediment-water interface are therefore sites of elevated decomposition not only because of availability of reactive substrate, but also because of the enhanced solute transport resulting from irrigation and physical proximity to the overlying water reservoir. Because the stimulation effects in this context result from general solute exchange and not simply oxidant supply, areas immediately adjacent to inhabited and irrigated regions should experience modest enhancement (observed in bioturbated microcosms, (e.g. Aller, 1978; Aller and Yingst, 1985; Kristensen and Blackburn, 1987;

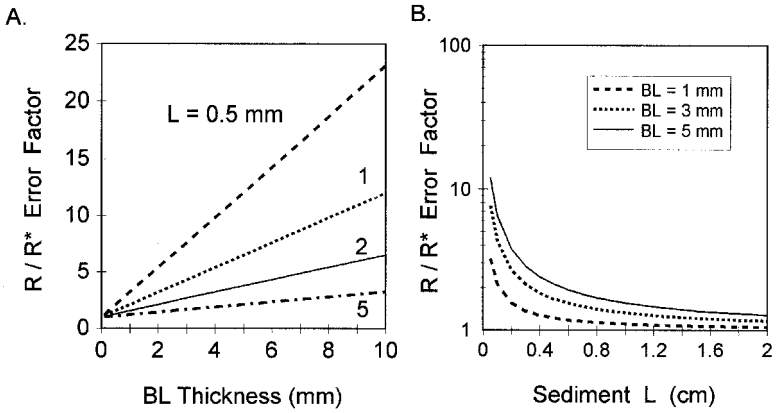

Figure 18. The reaction rate calculated from pore water—overlying water concentration differences is a function of diffusive boundary layer thickness (Eq. 6). (A). Relative rate calculation error of no BL case to BL case when boundary layer varies from 0 to 1 cm for fixed sediment plug thicknesses. (B). Relative rate calculation error increases with decreasing sediment L at fixed boundary layer thicknesses. These errors likely accentuate, but are not exclusively responsible for, the apparent increases in remineralization with decreasing sediment thickness.

Anderson and Kristensen, 1991), as should regions subject to exchange by direct biogenic or physical advection (Pedersen, 1982; Eckman, 1985).

It is important to recognize that the present experiments were entirely anoxic, and that under oxygenated overlying water conditions the eventual net solute exchange with overlying water may be strongly modified by boundary oxidized zones and reactions such as nitrification, adsorption, or metal oxidation. Such coupled redox processes should also be stimulated by increased net reactions in surrounding anoxic zones (i.e., supply of reduced reactants).

b. Factors determining net reaction rates

The dependence of net reaction rates on transport scale presumably reflects changing balances between competing reactions and processes that vary as a function of concentrations of reactants, products, or inhibiting components. Three possible simple quantitative cases are considered here as representative end-member conceptual examples capable of mimicing the net reaction patterns: coupled remineralization—biological uptake, coupled remineralization—abiogenic precipitation, and remineralization—inhibiting metabolite interactions.

When oxidants are in excess, the net decomposition of sedimentary organic carbon compounds is typically quantified phenomenologically using a first order kinetic relation (Berner, 1980):

$$\frac{d\hat{C}}{dt} = -k\hat{C} \tag{7}$$

where $\hat{C}$ = reactive organic carbon concentration, and k = pseudo first-order rate constant. The rates of remineralization of the minor constituents of organic matter, such as N, P, and I, are stoichiometrically related to the particular C_{org} pools undergoing decomposition. This is a practically useful but misleadingly simple formulation. In the original use of relation (7) in sedimentary modeling, the value of k was assumed to reflect the net result of a range of decomposition processes, and to be a function of a variety of environmental and biological conditions, in addition to the nature of the organic substrate (Berner, 1964; 1974). Consistent with such a definition, apparent magnitudes of k are often determined from net changes in the distributions of reactants (e.g. C_{org}, $SO_4^=$) or products (e.g. ΣCO_2, NH_4^+). However, many recent conceptual interpretations have come to emphasize or consider k largely an intrinsic function of the organic compounds involved, their physical associations, or available oxidants (reviewed in: Boudreau and Ruddick, 1991; Hedges and Keil, 1995). The reactive organic pool, $\hat{C}$, can also be a function of these very same factors (Mayer, 1994; Sun *et al.,* 1993; Hedges and Keil, 1995). Interactions between metabolic processes associated with reactive pools may themselves result in changes in net values of k or C (Canfield, 1994), and biogenic and abiogenic synthetic reactions also continuously alter the reactive pool (Paul and van Veen, 1978). As shown subsequently, in the present context, the apparent variation of net remineralization rate of C_{org} or nutrients as a function of diffusion scale can be interpreted in terms of concentration dependent reactions representing either changes in factors such as k or $\hat{C}$, changes in rates of coupled reactions such as microbial growth and uptake, changes in inhibitory solutes, or, most likely, simultaneous changes in all factors.

Remineralized components such as NH_4^+ are subject to substantial reincorporation into sedimentary microbial biomass for maintanence or growth (Paul and van Veen, 1978; Blackburn, 1979; Rice and Hanson, 1989). Assuming that such uptake can be represented by a Michaelis-Menten or Monod growth kinetic form (e.g., Fenchel and Blackburn, 1979; Bailey and Ollis, 1986), the net remineralization of NH_4^+, for example, is given by:

$$R_N = \sum_j \hat{R}_{N,j} - \frac{v_{max} C_N}{K_m + C_N} \tag{8}$$

where the net NH_4^+ production rate, R_N, is determined by summed solid phase decomposition terms stoichiometrically related to C_{org} components (j) through an equation like (7), ($\hat{R}_N \propto k\hat{C}$), C_N = dissolved concentration, v_{max} = saturated uptake rate, and K_m = half saturation concentration for NH_4^+. If, for purposes of illustration and simplicity, the production rate of NH_4^+ is assumed independently fixed by the nature of the organic substrate or a steady state (temporarily) bacterial population, then the net rate will vary only as a function of C_N, resulting in a dependence on diffusion scale comparable to that observed (Fig. 19) (reversible adsorption is ignored). As noted subsequently, the total production rate could also vary simultaneously with uptake (e.g., apparent value of k varies), and result in similar patterns. The closed incubations give a measure of $\Sigma\hat{R} - v_{max}$. Although apparently no values of K_m for natural populations of sedimentary bacteria have

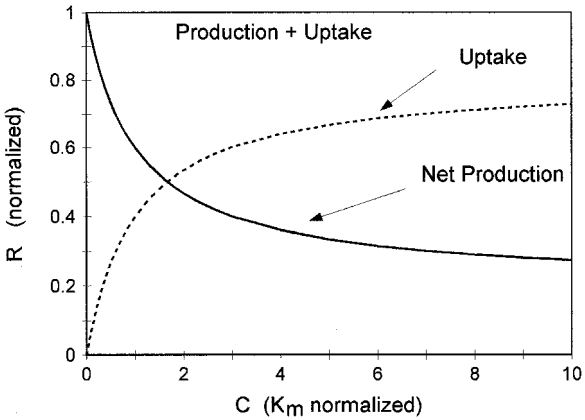

Figure 19. Changing balances between production and uptake as a function of concentration (proportional to diffusion scale) can result in net remineralization patterns similar to those observed (Eq. (8)). In this example case the value of R is normalized to the maximum production rate (no uptake), C is normalized to the uptake concentration at half-maximum (K_m), and uptake is assumed to be as much as 80% of produced solute.

been reported, fits to the present experimental data (assuming a constant total production rate) indicate that 10–20 μM may be reasonable for NH_4^+ (fits of Eq. (8) to 6 experiments give: $K_m \sim 11 \pm 4$ μM).

If reincorporation into bacterial biomass were a significant control on the observed net rate pattern, apparent stoichiometric relations between dissolved constituents should change as a function of diffusion scale, or until natural populations adapt their uptake rates to new conditions. The ratios of v_{max} values for individual elements would reflect stoichiometric ratios in new biomass. Some evidence for differential uptake comes from the relations between N/P and I/N production rate ratios as a function of transport scale or equivalently, concentration (Figs. 4 and 20). The net stoichiometric production ratio apparently changes as a function of transport scale or concentration. At the smaller scales these changes presumably reflect the stronger fractionation of P relative to N into bacterial biomass (C/P $\sim$ 30; C/N $\sim$ 5) compared to phytoplankton sources (C/P $\sim$ 106; C/N $\sim$ 6.6), and possibly, N relative to I (bacterial C/I $\sim$?). At the larger diffusion scales, dissolved concentrations are higher and additional reactions such as abiogenic mineral precipitation may alter net release (e.g. P mineral precipitation).

Mn^{++} is an example of a solute produced directly or indirectly during organic matter decomposition, and subject to abiogenic mineral precipitation rather than significant incorporation into biomass. Assuming that Mn^{++} is released stoichiometrically with respect to C_{org} oxidation, and that reprecipitation of a reduced Mn phase follows pseudo-first order kinetics, the net production rate, R_{Mn}, resulting from remineralization

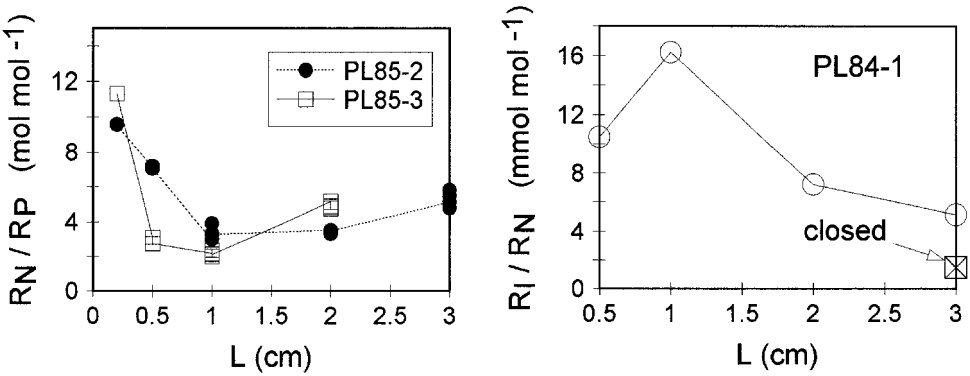

Figure 20. Apparent changes in net production stoichiometries of N/P and I/N occur with diffusion scale. These differences may result from varying balances between production and uptake reactions (Eq. (8), Fig. 19) with different elemental fractionations (e.g. planktonic source versus bacterial biomass uptake).

and abiogenic precipitation can be approximated as:

$$R_{\mathrm{Mn}} = \sum_j \hat{R}_{\mathrm{Mn},\,j} - k_{\mathrm{Mn}} C_{\mathrm{Mn}} \tag{9}$$

Where: $\hat{R}_{\mathrm{Mn},\,j}$ is the production of Mn^{++} from the summed solid phase decomposition terms stoichiometrically related to C_{org} components (j) through Eq. (7); k_{Mn} is a pseudo-first order precipitation rate constant, and C_{Mn} is the dissolved Mn^{++} concentration. An analytical solution for the dependence of net R_{Mn} on L at constant C_T can be readily obtained by substitution of (9) into model equations (1), giving a C_{ss} for use in Eq. (3) of:

$$C_{ss} = \sum_j \hat{R}_{\mathrm{Mn},\,j}/k_{\mathrm{Mn}} + \left(C_T - \sum_j \hat{R}_{\mathrm{Mn},\,j}/k_{\mathrm{Mn}} \right) \tanh\,(\sigma L)/\sigma L \tag{10a}$$

$$\sigma = \sqrt{k_{\mathrm{Mn}}/D_S}. \tag{10b}$$

For realistic ranges of k_{Mn} and $\Sigma \hat{R}_{\mathrm{Mn},j}$, and the practical limits on L used here, this function (when substituted into Eq. (3)) can result in nearly the same general scaling behavior of net production rates with L as does a relation such as Eq. (8). However, at larger scales the calculated net production rate, R_{Mn}, eventually becomes zero, and the predicted Mn^{++} concentrations may be excessively low due to lack of an equilibrium or kinetic bound in the simple example model equation used here (Fig. 21).

It is possible that the apparent response of decomposition activity to transport scale results from removal of inhibiting solutes such as reduced metabolites, as suggested by the examples of Figure 7. As transport scale decreases, the build-up of metabolic products and reaction inhibitors must also decrease, likely resulting in an overall increase in decomposition rate at a fixed value of biomass. If relaxation of inhibitory effects promotes bacterial

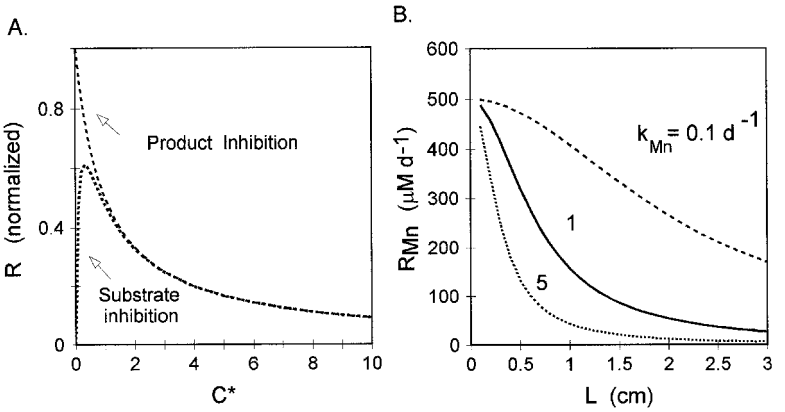

Figure 21. Reaction inhibition or backreactions (Eqs. 9–12) can also produce the relative net reaction rate patterns observed as a function of diffusion scale. (A) Example distributions of net reaction rates potentially resulting from product (Eq. 11) or substrate inhibition (Eq. 12). In this case, the relative concentration of inhibitor i is represented by the normalized parameter $C^* = C/K_i$ (see Eq. 10,11). The K_m/K_i ratio for substrate inhibition is assumed to be 0.1 in the present example. (B). Concentration dependent backreactions into inorganic precipates can also produce relative rate patterns as a function of diffusion scale similar to those observed. In these cases, various first order rate constants (0.1–5 d^{-1}) are assumed to govern Mn^{++} precipitation. Model equations (1, 3, 9,10) are used to calculate the net Mn^{++} production rate as a function of L.

growth, then net remineralization may also change as a result of biomass increase under more favorable conditions. In either scenario, the value of k in Eq. (7) would then appear to be dependent on transport regime. There is no generally-accepted functional dependence of biologically-mediated reaction rates on dissolved inhibitors in natural sediments, and previous work on inhibitory metabolites is largely restricted to extreme conditions in anaerobic digestors (e.g., Kaspar and Wuhrman, 1978; Hanaki *et al.,* 1981; Hansson and Molin, 1981; Jarrell *et al.,* 1987). In the present case, we utilize the basic inhibition function used in chemical reaction engineering and enzyme kinetics to describe metabolic substrate and product inhibition (Humphrey, 1972; Bailey and Ollis, 1986; Van Cappellen *et al.,* 1993). Again using NH_4^+ production as an example:

$$R_N = \frac{\sum_j \hat{R}_N}{1 + (C^*)} \tag{11}$$

In this case, the particular reaction inhibiting solute, C_i, is assumed normalized to an inhibition constant K_i, ($C^* = C_i/K_i$). The dependence of net reaction rate on inhibiting solute concentration can readily result in a net reaction rate—transport scale pattern comparable to that observed (Fig. 21). Obviously there may be multiple inhibitors (e.g., Jørgensen, 1983), and only the simplest example is considered here. Single substrate inhibition (inhibition constant K_i), for example, can result in net reaction functions such as

(12) and variants thereof:

$$R(C) = \frac{v_{max}C}{K_m + C + \dfrac{C \cdot C}{K_i}}. \tag{12}$$

These relationships reflect initial stimulation, followed by progressive inhibition of rate as a function of the same substrate. The effects of net biomass increases due to more favorable transport conditions are not quantitatively considered here, but would also result in an apparent increase in the effective value of k (e.g., v_{max}).

Additional processes may also promote enhanced or optimal decomposition in thinner, efficiently-exchanged sediment layers adjacent to fluid reservoirs. It is possible under some conditions that diffusion of reactive DOC from overlying water into sediment could result in greater supply of substrate to surficial zones, and thus cause volumetrically higher remineralization rates in thin, surfacemost layers. Such a case might occur environmentally, for example, in intertidal areas where DOC-rich waters draining marshes pass over bioturbated (irrigated) deposits. Desorption of decomposable organics may also provide an additional substrate flux in diffusively open sediment, stimulating total microbial activity (Keil *et al.,* 1994).

Although direct interactions and the coupling of transport with bacterial populations, metabolic activity, and dissolved reactants or products have been emphasized in our interpretations, it is also possible that changes in conditions associated with the transport regime may modify additional biological properties affecting remineralization. For example, increased solute exchange and lowered metabolite build-up could conceivably influence potential bacterial grazers such as protozoa or nematodes that are generally resistant or adapted to anoxic conditions but which might find lowered metabolite concentrations, such as characterize thin plugs, particularly favorable (e.g. Alkemade *et al.,* 1992; Giere, 1992; Hendelberg and Jensen, 1993). Enhanced grazing might thus correlate with transport scale, and help modify metabolic activity and net remineralization rates in the general manner observed; however, concomitantly increased bacterial biomass such as found in the present experiments would not be expected to accompany increased grazing (Fig. 13).

The major conclusion is that a range of quantitative conceptual models indicate that the phenomenological dependence of net reaction rates on transport scaling (irrigation) can be explained in multiple nonexclusive ways. In fact, the present data suggest that components of most if not all of the considered factors contribute simultaneously to the observed patterns, depending more or less on the particular solute involved. Relative concentrations of solid phase reactants (N,P) and the production of ΣCO_2 are consistent with higher absolute rates of decomposition as diffusive openness increases (Figs. 5,10,11). That is, with the conclusion that the effective value of k depends on environmental conditions, and on removal of metabolic inhibitors, and/or provision of reactive DOC from external and internal desorption sources. Multiple indicators of microbial activity also imply that

absolute activity increases with diffusive openness. The patterns of change in stoichiometric release ratios, along with previous work indicating substantial reincorporation of remineralized constituents into biomass (e.g., Blackburn, 1979; Reichardt, 1988; Rice and Hanson, 1989) suggest that balances between remineralization and uptake or abiogenic precipitation contribute to the observed patterns. Relatively greatest loss of Mn (not a significant biomass component) from thinnest plugs is direct evidence that concentration-dependent precipitation reactions and abiogenic retention of reaction products are decreased in diffusively open sediment. It should also be clear that in the limit of small scales or dilution, all rates must become vanishingly small, implying that an optimal scaling for maximal volumetric rates exists. Also, as emphasized previously, the presence of oxidized zones and coupled redox reactions can substantially modify the eventual sediment-water flux and reaction balances with changing transport scaling.

The solid phase P distributions are particularly revealing because of the previous documentation of large differences in P_{inorg} and P_{org} patterns in rocks derived from bioturbated and nonbioturbated sediments ($P_{org}/\Sigma P$ bioturbated $\sim$ 2–3$\times$ nonbioturbated; Ingall *et al.,* 1993). The present experiments demonstrate that under entirely anoxic conditions (e.g., away from oxidized burrow walls), the diffusive openness caused by irrigation promotes microbial synthesis of organic P during enhanced metabolic activity and growth, and results in greater retention of P_{org} relative to P_{inorg} in biologically irrigated deposits (Fig. 11). In fact, the P distribution differences observed under the experimentally diffusively open and closed conditions are comparable in magnitude to those found between bioturbated and nonbioturbated sedimentary rocks (e.g., $P_{org}/\Sigma P$ open plugs $\sim$ 1.5–2$\times$ closed; Fig. 11).

These results indicate that simple alterations in the spacing of individual burrow structures in sediments or the specific geometry of burrow sections are likely to have significant localized effects on microbial populations, net diagenetic reactions, and elemental cycling due solely to changes in diffusive transport. Apparent small changes in burrow geometries are likely to have significant impacts on reaction balances. It is clear that the coupling between macrofauna, bacteria, and diagenetic processes remains a rich, and largely unexplored, area of sedimentary research.

5. Conclusions

Net anoxic remineralization rates of organic matter increase regularly with increasing diffusive exchange or, equivalently, macrofaunal burrow spacing and irrigation intensity. Sedimentary constituents such as Mn^{++}, that are directly or indirectly coupled to organic matter decomposition, also show increases in net anoxic production rates and release with increased diffusive exchange (decreased transport scale or burrow spacing).

The relationships between net rates and solute exchange result in part from changes in balances between production and consumption reactions such as microbial uptake and abiogenic precipitation. Back reactions (biomass uptake, precipitation) decrease in relative importance to production reactions as solute concentrations decrease with transport scale.

However, total remineralization rates also increase with diffusive exchange, as indicated by increased microbial activity and changes in solid phase compositions (N,P,Mn), implying that loss of inhibiting metabolites or provision of dissolved reactants from overlying water or desorption are also important factors.

The net rate of sedimentary organic matter decomposition is controlled by the nature of the reductant or oxidant pools but is also a function of the environmental transport regime determined by a variety of physical or biological processes (e.g. metabolic solute exchange during irrigation).

Remineralization and elemental cycling in sediments are closely coupled to the solute and particle transport regime in surface sediment. Macrofauna likely manipulate solute transport, microbial activity, and diagenetic reaction balances through burrow spacing patterns and functional geometry.

Acknowledgments. The experimental results excerpted here were obtained at various times over a span of many years at SUNY Stony Brook, University of Chicago, Belle Baruch Marine Laboratory (Univ. S. Carolina), and Skidaway Institute of Oceanography (Savannah, Georgia). Many individuals aided at various times both in the field and laboratory. In particular, thanks to W. Ullman, R. Nelson, S. Dougherty, D. Allen, A. Ray, J. Mackin, M. Kino, L. Jasper, C. Gallup, T. (McGrath) Tromp, P. Rude, M. Jacobsen, S. Wirick, Q. Xia, I. Stupakoff, N. Soukas, M. Green, and E. Breuer. P. Kemp performed the RNA analyses. This work was supported by NSF grant no. OCE9314132 and predecessors. This is MSRC contribution no. 1110. We dedicate this paper in memory of our good friend and colleague, the late Qing Xia.

REFERENCES

Alkemade, R., A. Wielemaker, S. A. de Jong and A. J. J. Sandee. 1992. Experimental evidence for the role of bioturbation by the marine nematode *Diplolaimella dievengatensis* in stimulating the mineralization of *Spartina anglica* detritus. Mar. Ecol. Prog. Ser., *90,* 149–155.

Aller, R. C. 1978. Experimental studies of changes produced by deposit feeders on pore water, sediment, and overlying water chemistry. Amer. J. Sci., *278,* 1185–1234.

—— 1982. The effects of macrobenthos on chemical properties of marine sediment and overlying water, *in* Animal-Sediment Relations, P. L. McCall and M. J. S. Tevesz, eds., Plenum, NY, 53–102.

—— 1983. The importance of the diffusive permeability of animal burrow linings in determining marine sediment chemistry. J. Mar. Res., *41,* 299–322.

—— 1994. Bioturbation and remineralization of sedimentary organic matter: effects of redox oscillation. Chem. Geol., *114,* 331–345.

Aller, R. C. and J. E. Mackin. 1989. Open-incubation, diffusion methods for measuring solute reaction rates in sediments. J. Mar. Res., *47,* 411–440.

Aller, R. C. and J. Y. Yingst. 1985. Effects of the marine deposit-feeders *Heteromastus filiformis* (Polychaeta), *Macoma balthica* (Bivalvia), and *Tellina texana* (Bivalvia) on averaged sedimentary solute transport, reaction rates, and microbial distributions. J. Mar. Res., *43,* 615–645.

Andersen, F.Ø. and E. Kristensen. 1991. Effects of burrow macrofauna on organic matter decomposition in coastal marine sediments. Symp. Zool. Soc. Lond., *63,* 69–88.

Aspila, K. I., H. Agemian and A. S. Y. Chau. 1976. A semi-automatic method for the determination of inorganic, organic and total phosphate in sediments. Analyst., *101,* 187–197.

Bailey, J. E. and D. F. Ollis. 1986. Biochemical Engineering Fundamentals, McGraw-Hill, 984 pp.

Berner, R. A. 1964. An idealized model of dissolved sulfate distribution in recent sediments. Geochim. Cosmochim. Acta, *28,* 1497–1503.

—— 1974. Kinetic models for the early diagnesis of nitrogen, sulfur, phosphorus, and silicon in anoxic marine sediments, *in* The Sea, *5,* E. D. Goldberg, ed., J. Wiley, NY, 427–450.

—— 1980. Early Diagenesis: A Theoretical Approach. Princeton University Press, Princeton, NJ, 241 pp.

Blackburn, T. H. 1979. Method for measuring rates of NH_4^+ turnover in anoxic marine sediments, using a 15N-NH_4^+ dilution technique. Appl. Environ. Micro. *37,* 760–765.

Boechker, H. T. S. and T. E. Cappenberg. 1994. A sensitive method using 4-Methylumbelliferyl-a-Cellobiose as a substrate to measure (1,4)-a-Glucanase activity in sediments. Appl. Environ. Micro., *60,* 3592–3596.

Boudreau, B. P. and B. R. Ruddick. 1991. On a reactive continuum representation of organic matter diagenesis. Amer. J. Sci., *291,* 507–538.

Bulleid, N. C. 1978. An improved method for the extraction of adenosine triphosphate from marine sediment and seawater. Limnol. Oceanogr., *23,* 174–178.

Canfield, D. E. 1994. Factors influencing organic carbon preservation in marine sediments. Chem. Geol., *114,* 315–329.

Chrost, R. J. 1991. Environmental control of the synthesis and activity of aquatic microbial ectoenzymes, *in* Microbial Enzymes in Aquatic Environments, R. J. Chrost, ed., Springer-Verlag, NY, 84–95.

Eckman, J. E. 1985. Flow disruption by an animal-tube mimic affects sediment bacterial colonization. J. Mar. Res., *43,* 419–435.

Fenchel, T. and T. H. Blackburn. 1979. Bacteria and Mineral Cycling, Academic Press, NY, 225 pp.

Giere, O. 1992. Benthic life in sulfidic zones of the sea—ecological and structural adaptations to a toxic environment. Verh. Dtsch. Zool. Ges., *85,* 77–93.

Goto, K., T. Komatsu and T. Furukawa. 1962. Rapid colorimetric determination of managanese in waters containing iron. Analytica Chemica Acta, *27,* 331–334.

Hall, P. O. J. and R. C. Aller. 1992. Rapid, small-volume, flow injection analysis for ΣCO_2 and NH_4^+ in marine and freshwaters. Limnol. Oceanogr., *37,* 1113–1119.

Hanaki, K., T. Matsuo and M. Nagase. 1981. Mechanism of inhibition caused by long-chain fatty acids in anaerobic digestion process. Biotech. Bioeng., *23,* 1591–1610.

Hansson, G. and N. Molin. 1981. End product inhibition in methane fermentations: effects of carbon dioxide and methane on methanogenic bacteria using acetate. European J. Appl. Microbiol. Biotechnol., *13,* 236–241.

Hedges, J. I. and R. G. Keil. 1995. Sedimentary organic matter preservation: an assessment and speculative synthesis. Mar. Chem., *49,* 81–115.

Hendelberg, M. and P. Jensen. 1993. Vertical distribution of the nematode fauna in a coastal sediment influenced by seasonal hypoxia in the bottom water. Ophelia, *37,* 83–94.

Hoppe, H. G. 1993. Use of fluorogenic model substrates for extra cellular enzyme activity (EEA) measurement of bacteria, *in* Aquatic Microbial Ecology, P. F. Kemp, B. F. Sherr, E. B. Sherr and J. J. Cole, eds., Lewis Publ., Boca Raton, FL, 423–432.

Humphrey, A. E. 1972. The kinetics of biosystems: A review, *in* Chemical Reactor Engineering, R. F. Gould, ed. Am. Chem. Soc. Adv. Chem. Series, *109,* 630–650.

Ingall, E. D., R. M. Bustin and P. Van Cappellen. 1993. Influence of water column anoxia on the burial and preservation of carbon and phosphorus in marine shales. Geochim. Cosmochim. Acta, *57,* 303–316.

Jarrell, K. F., M. Saulnier and A. Ley. 1987. Inhibition of methanogenesis in pure cultures by

ammonia, fatty acids, and heavy metals, and protection against heavy metal toxicity by sewage sludge. Can. J. Microbiol., *33,* 551–554.

Jorgensen, B. B. 1983. Processes at the sediment-water interface, *in* The Major Biogeochemical Cycles and Their Interactions, B. Bolin and R. B. Cook, eds., SCOPE 21, J. Wiley and Sons, Chichester, 477–509.

Jørgensen, B. B. and N. P. Revsbech. 1985. Diffusive boundary layers and the oxygen uptake of sediments and detritus. Limnol. Oceanogr., *30,* 111–122.

Kaspar, H. F. and K. Wuhrmann. 1978. Product inhibition in sludge digestion. Microbial Ecology, *4,* 241–248.

Keil, R. G., D. B. Montlucon, F. G. Prahl and J. I. Hedges. 1994. Sorptive preservation of labile organic matter in marine sediments. Nature, *370,* 549–552.

Kemp, P. F. 1995. Can we estimate bacterial growth rates from ribosomal RNA content? *in* Molecular Ecology of Aquatic Microbes, I. Joint, ed., NATO ASI Series, G38, Springer Verlag, Berlin, 279–302.

Kemp, P. F., S. Lee and J. LaRoche. 1993. Evaluating bacterial activity from cell-spediric ribosomal RNA content measured with oligonucleotide probes, *in* Aquatic Microbial Ecology, B. F. Sherr, E. B. Sherr and J. J. Cole, eds., Lewis Publ., Boca Raton, FL, 415–422.

King, G. M. 1986. Inhibition of microbial activity in marine sediments by a bromophenol from a hemichordate. Nature (London), *323,* 257–259.

Kristensen, E., R. C. Aller and J. Y. Aller. 1991. Oxic and anoxic decomposition of tubes from the burrowing sea anemone *Ceriantheopsis americanus:* Implications for bulk sediment carbon and nitrogen balance. J. Mar. Res., *49,* 589–617.

Kristensen, E. and T. H. Blackburn. 1987. The fate of organic carbon and nitrogen in experimental marine sediment systems: influence of bioturbation and anoxia. J. Mar. Res., *45,* 231–257.

Lee, S. H., C. Malone and P. F. Kemp. 1993. Use of multiple 16S rRNA-targeted fluorescent probes to increase signal strength and measure cellular RNA from natural planktonic bacteria. Mar. Ecol. Prog. Ser., *101,* 193–201.

Li, Y.-H. and S. Gregory. 1974. Diffusion of ions in sewater and in deep-sea sediments. Geochim. Cosmochim. Acta, *38,* 703–714.

Mackin, J. E. and R. C. Aller. 1984. Ammonium adsorption in marine sediments. Limnol. Oceanogr., *29,* 250–257.

Mayer, L. M. 1994. Surface area control of organic carbon accumulation in continental shelf sediments. Geochim. Cosmochim. Acta, *58,* 1271–1284.

Mayer, M. S., L. Schaffner and W. M. Kemp. 1995. Nitrification potentials of benthic macrofaunal tubes and burrow walls: effects of sediment NH_4^+ and animal irrigation behavior. Mar. Ecol. Prog. Ser., *12,* 157–169.

Meyer-Reil, L. A. 1986. Measurement of hydrolytic activity and incorporation of dissolved organic substrates by microorganisms in marine sediments. Mar. Ecol. Prog. Ser., *31,* 143–149.

Paul, E. A. and J. A. van Veen. 1978. The use of tracers to determine the dynamic nature of organic matter. Trans. 11th Int. Congr. Soil Sci., *3,* 61–89.

Pedersen, K. 1982. Factors regulating microbial biofilm development in a system with slowly flowing seawater. Appl. Environ. Micro., *44,* 1196–1204.

Pelegri, S. P., L. P. Nielsen and T. H. Blackburn. 1994. Denitrification in estuarine sediment stimulated by the irrigation activity of the amphipod *Corophium volutator.* Mar. Ecol. Prog. Ser., *105,* 285–290.

Reichardt, W. 1988. Impact of bioturbation by *Arenicola marina* on microbiological parameters in intertidal sediments. Mar. Ecol. Prog. Ser., *44,* 149–158.

Rhoads, D. C. 1974. Organism-sediment relations on the muddy sea floor. Oceanogr. Mar. Biol. Ann. Rev., *12,* 263–300.

Rice, D. L. and R. B. Hanson. 1989. A kinetic model for detritus nitrogen: role of the associated bacteria in nitrogen accumulation. Bull. Mar. Sci., *35,* 326–340.

Rosenfeld, J. 1979. Ammonium adsorption in nearshore anoxic sediments. Limnol. Oceanogr., *24,* 356–364.

Ruttenberg, K. C. 1992. Development of a sequential extraction method for different forms of phosphorus in marine sediments. Limnol. Oceanogr., *37,* 1460–1482.

Santschi, P. H., R. F. Anderson, M. Q. Fleisher and W. Bowles. 1991. Measurements of diffusive sublayer thicknesses in the ocean by alabaster dissolution, and their implications for the measurements of benthic fluxes. J. Geophys. Res., *96*(C6), 10,641–10,657.

Solorzano, L. 1969. Determination of ammonia in natural waters by the phenolhypochlorite method. Limnol. Oceanogr., *14,* 799–801.

Strickland, J. D. H. and T. R. Parsons. 1969. A practical handbook of sea water analysis: Canada Fish. Res. Bd, Bull., *167,* 311 pp.

Sun, M-Y., C. Lee and R. C. Aller. 1993. Anoxic and oxic degradation of ^{14}C-labeled chloropigments and a ^{14}C-labeled diatom in Long Island Sound sediments. Limol. Oceanogr., *38,* 1438–1451.

Ullman, W. J. and R. C. Aller. 1982. Diffusion coefficients in nearshore marine sediments. Limnol. Oceanogr., *27,* 552–556.

Van Cappellen, P., J.-F. Gaillard and C. Rabouille. 1993. Biogeochemical transformation in sediments: kinetic models of early diagenesis, *in* NATO-ARW Interactions of C, N, P and S Biogeochemical Cycles and Global Change, R. Wollast, L. Chou and F. Mackenzie, eds., Springer, NY, 401–445.

Watson, S. W., T. J. Novitsky, H. L. Quinby and F. W. Valois. 1977. Determination of bacterial number and biomass in the marine environment. Appl. Environ. Microbiol., *33,* 940–946.

Woese, C. R. 1987. Bacterial evolution. Microbiol. Rev., *51,* 221–271.

Woodin, S. A., R. L. Marinelli and D. E. Lincoln. 1993. Biogenic brominated aromatic compounds and recruitment of infauna. J. Chem. Ecol., *19,* 517–530.

Received: *19 August, 1997;* revised: *13 April, 1998.*